Journal of Magnetic Resonance 212 (2011) 394–401

Contents lists available at SciVerse ScienceDirect

Journal of Magnetic Resonance

journal homepage: www.elsevier.com/locate/jmr

Emulation of petroleum well-logging $D - T_2$ correlations on a standard benchtop spectrometer

J. Mitchell [a], E.J. Fordham [b,*]

[a] Department of Chemical Engineering and Biotechnology, University of Cambridge, Pembroke Street, Cambridge CB2 3RA, United Kingdom
[b] Schlumberger Cambridge Research, High Cross, Madingley Road, Cambridge CB3 0EL, United Kingdom

ARTICLE INFO

Article history:
Received 30 June 2011
Revised 22 July 2011
Available online 2 August 2011

Keywords:
$D - T_2$ correlation
Diffusion-editing
Pulsed field gradient
Fixed field gradient
Reservoir rocks
Rock core analysis
Fluid characterisation

ABSTRACT

An experimental protocol is described that allows two-dimensional (2D) nuclear magnetic resonance (NMR) correlations of apparent diffusion coefficient D_{app} and effective transverse relaxation time $T_{2,eff}$ to be acquired on a bench-top spectrometer using pulsed field gradients (PFG) in such a manner as to emulate $D_{app} - T_{2,eff}$ correlations acquired using a well-logging tool with a fixed field gradient (FFG). This technique allows laboratory-scale NMR measurements of liquid-saturated cored rock to be compared directly to logging data obtained from the well by virtue of providing a comparable acquisition protocol and data format, and hence consistent data processing. This direct comparison supports the interpretation of the well-logging data, including a quantitative determination of the oil/brine saturation. The $D - T_2$ pulse sequence described here uses two spin echoes (2SE) with a variable echo time to encode for diffusion. The diffusion and relaxation contributions to the signal decay are then deconvolved using a 2D numerical inversion. This measurement allows shorter relaxation time components to be probed than in conventional diffusion measurements. A brief discussion of the numerical inversion algorithms available for inverting these non-rectangular data is included. The PFG-2SE sequence described is well suited to laboratory-scale studies of porous media and short T_2 samples in general.

1. Introduction

One-dimensional (1D) transverse T_2 relaxation time distributions are used as a discriminator of fluid type in nuclear magnetic resonance (NMR) well-logging applications [1]. These measurements are conducted routinely at low magnetic field strengths ($B_0 \leqslant 50$ mT) and, in the case of well-logging tools, in the presence of a strong background magnetic field gradient. As such, chemical shift information cannot be obtained. Separation of signals arising from oil, gas, and brine fractions in the pore space relies on determining a characteristic T_2 relaxation time for each of the chemical species. In some cases, the separation of the T_2 components is complicated by the convolved dependence of the effective (observed) $T_{2,eff}$ on pore size and diffusion through the inhomogeneous magnetic field. Under such circumstances it is possible for light oil fractions to have the same $T_{2,eff}$ as brine. The addition of an apparent diffusion coefficient dimension in the two-dimensional (2D) $D_{app} - T_{2,eff}$ correlation experiment can provide the required discrimination of fluid types (referred to as "diffusion-editing") [2]. The apparent diffusion coefficient D_{app} is modified from the bulk fluid diffusion coefficient D_0 by the confining pore network. Analysis of $D_{app} - T_{2,eff}$ correlations can provide valuable discrimination of fluid type in complex rock formations where the T_2 relaxation time distribution alone would not yield sufficient information to interpret the well-log.

In NMR well-logging tools, the inherent magnetic field profile of the unilateral device provides a fixed magnetic field gradient ∇B_0 that can be used to measure D_{app}. Nuclear spins moving in a magnetic field gradient accumulate phase proportional to the distance travelled during the encoding time of the experiment. A distribution of such phase accumulations, resulting from a distribution of distances travelled, is observed as a reduction in the coherent signal derived from the excited spin ensemble. In the presence of this permanent gradient, a diffusion measurement is achieved simply by varying the echo time spacing of a spin echo [3].

Even with the advanced capabilities of modern NMR well-logging tools, it is still desirable to conduct complementary experiments in the laboratory on cored rock to support the down-hole results; see for example [4]. An equivalent $D_{app} - T_{2,eff}$ experimental protocol can be devised in the laboratory using the inhomogeneous stray field of a superconducting magnet [5]. Alternatively, permanent magnets can be constructed to have stray fields optimised for diffusion studies in very small samples [6]. However, these laboratory-scale stray field measurements have two significant limitations:

* Corresponding author.
E-mail address: fordham@cambridge.oilfield.slb.com (E.J. Fordham).

1090-7807/$ - see front matter © 2011 Elsevier Inc. All rights reserved.
doi:10.1016/j.jmr.2011.07.020

1. The inherent slice-selection of the gradient results in a loss of signal-to-noise ratio (SNR) due to the small sample volume that is far worse than in the logging tool.
2. Significant ^{19}F signal contamination will occur when per-fluorinated liquids in the core-plug confining system are selected by the gradient.

The same limitations apply when using a standard benchtop NMR spectrometer modified in such a manner as to provide a quasi-static magnetic field gradient of sufficient amplitude to emulate the performance of a well-logging tool.

It is desirable, therefore, to study rock core-plugs on the laboratory scale in a standard benchtop NMR spectrometer that does not have such a grossly inhomogeneous magnetic field profile. Here we describe a NMR sequence with pulsed field gradients (PFG) that emulates closely the fixed field gradient (FFG) $D_{app} - T_{2,\mathrm{eff}}$ measurement of a well-logging tool [7]. This sequence can be implemented on a commercial benchtop system without any special modifications. As the gradient is pulsed, none of the limitations associated with a fixed gradient apply, and signal is obtained from the whole core-plug. However, despite the equivalence of the diffusion-editing portion of the FFG and PFG sequences, some differences may exist in the data; notably, the source of the diffusion weighting in $T_{2,\mathrm{eff}}$ can differ. The lack of a static magnetic field gradient in the PFG case is a necessary workaround such that interpretation of the $T_{2,\mathrm{eff}}$ dimension may differ between the FFG and PFG results to account for the different source of diffusion weighting in each relaxation time analysis. In the FFG experiment, the static (background) magnetic field gradient of the logging tool can dominate, whereas in the PFG experiment magnetic susceptibility induced "internal gradients" will likely dominate over any magnetic field inhomogeneity during the $T_{2,\mathrm{eff}}$ measurement. For example, a typical logging tool background gradient is $g_0 \leqslant 50$ G cm^{-1} whilst the internal gradients observed in rocks can vary widely; for example, in [8] maximum internal gradients of $g_{\max} = 600$ G cm^{-1} were reported. In this work we have chosen to use Bentheimer sandstone, being unusual for a sand insomuch as the internal gradients are weak: at $\nu_0 = 2$ MHz, $g_{\mathrm{eff}} < 1$ G cm^{-1} [9], although such internal gradient strengths are not uncommon for limestones.

A variety of versatile diffusion measurements are available on benchtop spectrometers and a review of the more common implementations can be found in [10,11]. Of particular interest in studies of porous media is the so-called "Cotts-13" alternating pulsed gradient stimulated echo (APGSTE) sequence [12]. This pulse sequence is designed to limit the influence of background gradients on the diffusion experiment. This background gradient compensation is essential in intermediate to high-field NMR measurements of porous media, where the internal gradients can be significant. The consequences of measuring rock core-plugs at high field strengths have been discussed in [9]. However, the preference in laboratory studies of liquid saturated rocks is the use of low-field magnets ($B_0 < 0.1$ T) to ensure empirical comparability with well-logging tools. Pulse sequences such as the APGSTE are difficult to implement reliably on low-field magnets due to the inherent complications in the spin dynamics. Notably, the rf excitation pulses contain only a few cycles of rf leading to pulse imperfections, and the B_0 and B_1 fields are inhomogeneous compared to a superconducting magnet. Additionally, the stimulated echo introduces T_1 relaxation weighting [13]. It is desirable, therefore, to use a simple pulse sequence such as the original spin echo PFG experiment conducted by Stejskal and Tanner [14]. The inherent T_2 relaxation weighting can be ignored if the timing of the rf events (excitation and detection) remains constant and the gradient strength is incremented in successive acquisitions to encode for diffusion.

By contrast, it is necessary to maintain a constant gradient strength and increment the gradient pulse duration (hence rf event separation) in successive experiments to emulate a well-logging tool on a benchtop spectrometer. If conducting a 1D diffusion measurement in this manner, it is impossible to separate the contributions from diffusion and relaxation when multiple T_2 components are present. However, the implementation of a 2D numerical inversion allows the diffusion and relaxation exponents to be deconvolved [2]. The diffusion-editing measurement described in Section 2 is preferential in core analysis as it allows a direct comparison between well-logs and laboratory data. Example data are presented in Section 5 to demonstrate the capabilities of this technique. In general, the spin echo diffusion experiment described here allows shorter relaxation times to be probed than in conventional PFG experiments by virtue of the variable echo time spacing.

2. Pulse sequence

When describing pulse sequences, we follow the notation of Stejskal and Tanner [14] where δ is the gradient duration and Δ is the effective diffusion time (defined as the time between the leading gradient edges in PFG experiments).

We consider first the FFG double spin echo (FFG-2SE) pulse sequence as applied in the stray field of a unilateral NMR device such as a well-logging tool [3,8]. The timing diagram is shown in Fig. 1. The sequence utilises a pair of spin echoes with a variable echo spacing $t_{\mathrm{SE},i}$ (where i is the experiment index) to encode for diffusion in the first portion of the pulse sequence (the indirect data dimension). The intensity of the second spin echo is recorded as this is motion compensated, whereas the first spin echo is not [3]. In the second portion of the pulse sequence (the direct data dimension), T_2 relaxation data are acquired using a conventional

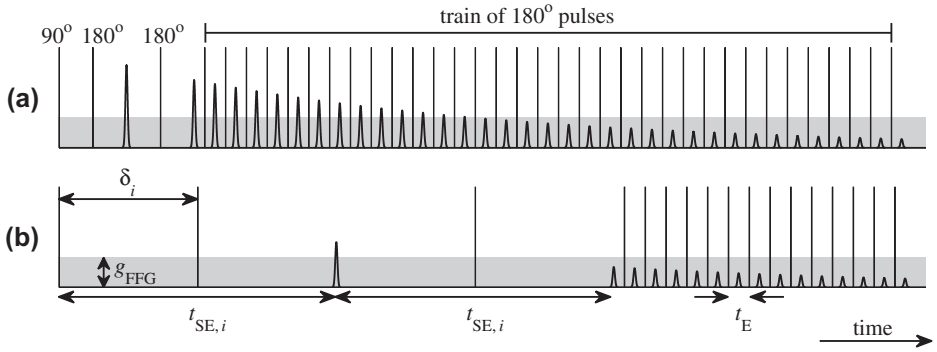

Fig. 1. FFG-2SE pulse sequence as implemented on unilateral NMR devices. A background gradient of amplitude g_{FFG} is present at all times; $t_{\mathrm{SE},i} = 2\delta_i$ is incremented in i successive experiments to encode for diffusion. Examples of (a) short and (b) long δ are shown. A train of n CPMG echoes with fixed echo spacing t_{E} are acquired after a time $2t_{\mathrm{SE},i}$ (echo trains shown here are truncated for clarity). The observed echoes are narrow due to spectral line broadening caused by the fixed gradient.

Carr–Purcell Meiboom–Gill (CPMG) train of echoes [15,16] with fixed echo spacing t_E sufficiently short so as to limit diffusion weighting in the inhomogeneous magnetic field. The spectral line of any sample will be broadened significantly by the fixed field gradient. As the signal is acquired in the presence of this gradient, the observed echoes are narrow and precise timing is required to ensure the echo amplitude is recorded accurately [3,17]. The constant gradient amplitude g_{FFG} is determined by the position of the sensitive volume in the stray magnetic field of the device. For well-logging tools, the gradient strength is in the range $g_{FFG} \approx 20 - 50\ \mathrm{G\,cm^{-1}}$, depending on the distance of excitation away from the magnet pole. In the FFG pulse sequence, the effective gradient duration is $\delta_i = t_{SE,i}/2 \equiv \Delta$. The gradient "area", which is of consequence to the diffusing spins, is therefore given by $\delta_i g_{FFG}$.

We now describe the equivalent PFG double spin echo (PFG-2SE) pulse sequence as shown in Fig. 2. The rf pulse timing is identical to the FFG pulse sequence; however, there is no fixed magnetic field gradient and instead the diffusion editing is achieved by applying gradient pulses between the rf events. Shaped gradient pulses reduce eddy-currents induced in the magnet poles by virtue of decreasing the rate of change of current dI/dt in the gradient coils compared to a square gradient pulse [11]. Trapezoidal gradient pulses are often used, although in the implementation shown in Fig. 2 we have chosen half-sine pulses out of personal preference. The gradient pulses are applied immediately after the rf events, although a gradient stabilisation delay is required prior to the next rf event; the duration of this delay will depend on the spectrometer hardware. Hence, $\delta_i < t_{SE,i}/2$ in this PFG-2SE sequence, while $\Delta \equiv t_{SE,i}/2$. To enable the PFG sequence to emulate the FFG sequence, the spins must experience the same effective gradient area. It is therefore necessary to apply the gradient pulses with a maximum amplitude g_{PFG} such that the area of the ith gradient pulse is equivalent to $\delta_i g_{FFG}$. In the case of half-sine gradient pulses,

$$g_{PFG}\int_0^{\delta_i} \sin\left(\frac{\pi t}{\delta_i}\right) dt \equiv \delta_i g_{FFG}. \tag{1}$$

In the PFG sequence, the echoes are not acquired in the presence of a field gradient; hence there will be no broadening of the spectral line. The acquired echoes are narrowed only by heterogeneities in B_0 imposed by the magnet hardware and magnetic susceptibility contrast in the sample. Numerous data points can therefore be obtained across the top of each echo, leading to an enhanced SNR compared to the echoes acquired in the presence of a gradient. Furthermore, it is possible to acquire an extra data row ($i = 0$) with no diffusion gradient in the PFG implementation (effectively a standard CPMG measurement). This extra data row corresponds to the theoretical FFG case where $\delta_0 \to 0$ and $t_{SE,0} \to t_E$; it is not physically possible to acquire these data in the FFG experiment. This addition in the PFG implementation allows a direct determination of the $T_{2,eff}$ distribution and hence improved separation of the convolved $T_{2,eff}$ and D_{app} distributions. The addition also means that shorter relaxation time components will be observed than in conventional PFG or FFG experiments.

3. Data processing

The diffusion-editing class of pulse sequences are unusual among NMR diffusion measurements in that both the echo time and gradient pulse duration vary. In general, the data processing is more convenient when the timings are constant, e.g. PFG sequences given in [8]. For the FFG-2SE pulse sequence shown in Fig. 1, the intensity (magnetisation m) of the second spin echo in the ith experiment will be given by

$$m(2t_{SE,i}) = m_0 \exp\left\{-\frac{1}{6}\gamma^2 g_{FFG}^2 D_{app} t_{SE,i}^3\right\} \exp\left\{-\frac{2t_{SE,i}}{T_{2,eff}}\right\}, \tag{2}$$

where γ is the gyromagnetic ratio of the spins and m_0 is the magnetisation at zero time. Likewise for the PFG-2SE pulse sequence with half-sine gradient pulses shown in Fig. 2,

$$m(2t_{SE,i}) = m_0 \exp\left\{-\gamma^2 g_{PFG}^2 D_{app} \frac{\delta_i^2 (2t_{SE,i} - \delta_i)}{\pi^2}\right\} \exp\left\{-\frac{2t_{SE,i}}{T_{2,eff}}\right\}. \tag{3}$$

A summary of modifications to the diffusion equation for different gradient pulse shapes can be found in [11]. From Eq. (3) the b-factor, defined in the diffusion exponent as $\exp\{-bD_{app}\}$, is

$$b = \gamma^2 g_{PFG}^2 \delta_i^2 \frac{(2t_{SE,i} - \delta_i)}{\pi^2}. \tag{4}$$

It is therefore obvious from Eqs. (2) and (3) that, due to the common variable $t_{SE,i}$ shared by the diffusion and relaxation exponents, the distribution of D_{app} cannot be determined unless the distribution of $T_{2,eff}$ is known. As such, 2D data processing is required to differentiate between the diffusion and relaxation contributions to the signal attenuation.

2D data are generated using the PFG or FFG spin echo sequences by incrementing the gradient duration δ_i and echo time $t_{SE,i}$ in the second (indirect) dimension and acquiring a train of n echoes in the first (direct) dimension. The data matrix then contains $n \times i$ complex data points, where $n \sim 10^4$ and $i \sim 32$, typically. These data are described by a 2D Fredholm integral equation of the first kind (in continuous functional form) as:

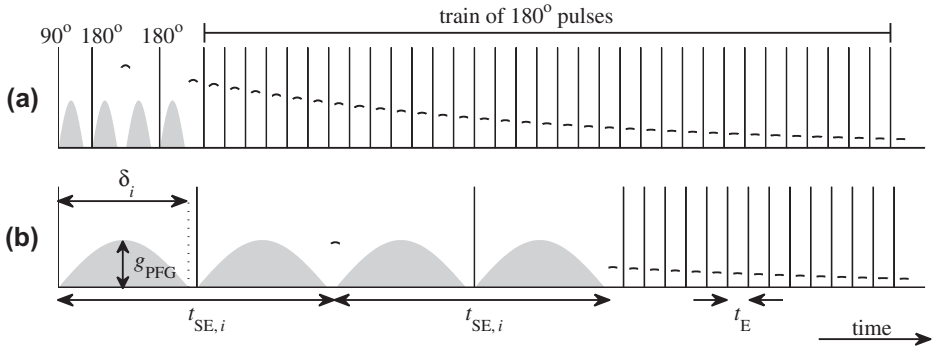

Fig. 2. PFG-2SE pulse sequence as implemented on a standard benchtop spectrometer. Gradient pulses of maximum amplitude g_{PFG} and duration δ_i are applied between the initial rf pulses; δ_i and $t_{SE,i}$ are incremented in i successive experiments to encode for diffusion. Examples of (a) short and (b) long δ are shown. A train of n CPMG echoes with fixed echo spacing t_E are acquired after a time $2t_{SE,i}$ (echo trains shown here are truncated for clarity). The observed echoes are broad, allowing multiple data points to be acquired from each echo and summed to improve the overall SNR.

$$\frac{m(2t_{SE}, nt_E)}{m(0,0)} = \int_0^\infty \int_0^\infty k_0(D_{app}, T_{2,\ eff}, 2t_{SE}, nt_E) \times f(D_{app}, T_{2,eff})\mathrm{d}(\log_{10} D_{app})\mathrm{d}(\log_{10} T_{2,eff}) + e(2t_{SE}, nt_E), \quad (5)$$

where m is the observed magnetisation, k_0 is a kernel function describing the ideal shape of the data, f is the required $D_{app} - T_{2,eff}$ correlation function, and e is the experimental error (noise). For the practical implementation of the numerical inversion required to determine f given m, the acquired data matrix **M** is stacked into the vector **m**, the required solution matrix **F** is obtained as the stacked vector **f**, and the kernel function is described by the matrix $\mathbf{K}_0$. Consequently, the experimental noise will also be a stacked vector **e**. As such, the Fredholm integral equation is written as

$$\mathbf{m} = \mathbf{K}_0\mathbf{f} + \mathbf{e}. \quad (6)$$

This Fredholm integral equation represents an ill-posed problem and regularisation (smoothing) is usually implemented to achieve a stable solution in the presence of noise. Regularisation is imposed by (1) forcing the solution to be non-negative, (2) limiting the fitting range of $T_{2,eff}$ and D_{app}, and (3) biasing the solution to be smooth. The smoothing can be achieved by a variety of similar numerical methods. In well-logging, data from the FFG pulse sequence are smoothed using the maximum entropy method [18]. Tikhonov regularisation following the method described by Butler et al. [19,20] is preferred for smoothing PFG data acquired on benchtop spectrometers. The maximum entropy method provides a rapid fit to the data with the level of smoothing determined by the SNR. However, the maximum entropy method cannot cope with systematic data errors specific to our experimental setup, whereas the Tikhonov regularisation introduces a tunable smoothing parameter that allows systematic errors to be overcome by increasing the degree of smoothing imposed on the solution. For ideal data (i.e. data that match the modelled form given in the kernel matrix), the two regularisation methods provide consistent and near identical solutions.

To simplify the data processing, we chose to make the variable substitution $t' = 2t_{SE,i} + nt_E$ [8]. Now the two dimensions of the experimental data matrix can be considered independent, although the dataset is no longer rectangular; see Fig. 3a. Tikhonov regularisation can be achieved efficiently if the data dimensions are separable (i.e. do not share a common variable) [20], as in the FFG or PFG data following the variable substitution. Under such conditions the kernel matrix $\mathbf{K}_0$ can be expressed as the Krönecker product $\mathbf{K}_0 = \mathbf{K}_2 \otimes \mathbf{K}_1$, where $\mathbf{K}_{1,2}$ are small compared to $\mathbf{K}_0$. However, this introduces a further complication because this implementation of the regularisation method can be applied only to rectangular data. Previously, data from the FFG spin echo pulse sequence have been inverted using this method by truncating the non-rectangular data matrix [8], as illustrated in Fig. 3b. This truncation is not desirable as the data points with the highest SNR are discarded from the fit. An alternative approach is to extrapolate the data to a rectangular matrix [21], Fig. 3c, although this extrapolation is likely to result in the creation of artificial short or long T_2 components.

Here, we chose to invert the data without forcing the data matrix to be rectangular. The inversion can be achieved by computing the entire $\mathbf{K}_0$ kernel matrix. Given the size of our example data matrix of $10^4 \times 32$ elements and a typical solution matrix of size 64×64 elements, $\mathbf{K}_0$ will contain $\sim 10^9$ elements. Therefore, it is computationally expensive to calculate and store $\mathbf{K}_0$. To reduce the size of the kernel matrix, a pre-processing data compression stage is added whereby the n echoes in each row are compressed to, say 32 elements, using window averages [22,23] as demonstrated in Fig. 4. A weighting matrix $\mathbf{W}_0$ then needs to be included

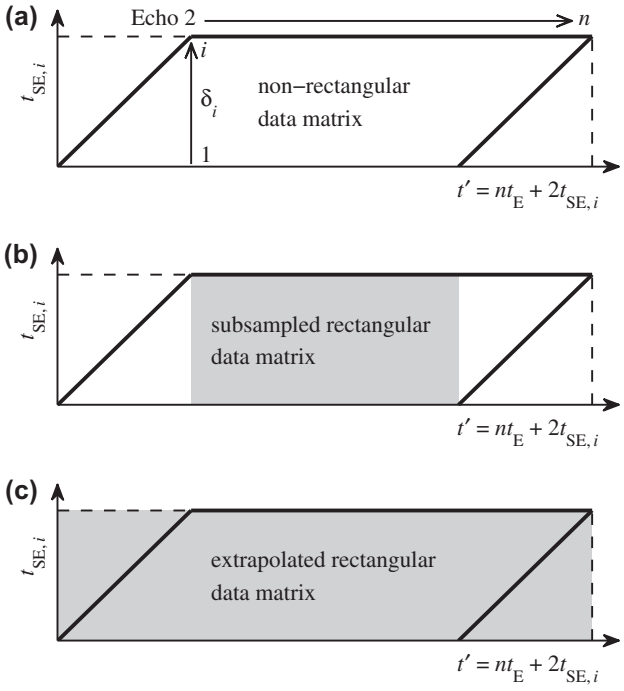

Fig. 3. (a) Non-rectangular arrays generated by the variable substitution $t' = 2t_{SE,i} + nt_E$ in data from PFG-2SE or FFG-2SE experiments. The gradient duration δ_i increases vertically and the number of echoes in the CPMG echo train increases horizontally. The maximum SNR is obtained in the bottom left corner where $i = 1$ and $n = 2$. Data can be (b) truncated or (c) extrapolated to provide a rectangular array.

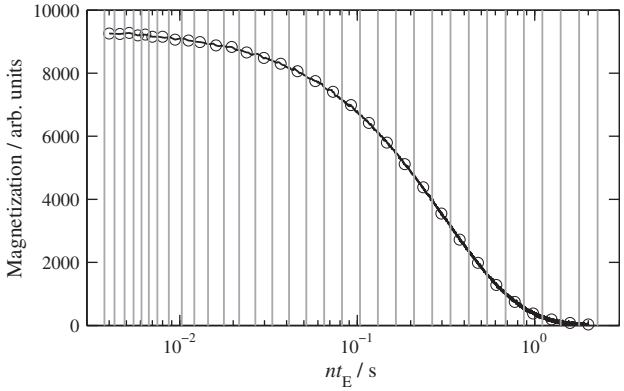

Fig. 4. Window averaging demonstrated on example CPMG data from a doped water phantom. The raw data (black line) are divided into logarithmically sized bins (vertical grey lines). The data points in each bin are averaged to provide the compressed data (circles). The width of the initial bins varies slightly to accommodate an integer number of data points. The SNR of the compressed data varies from point-to-point due to the increasing width of the bins. In this example, an input of $n \approx 3 \times 10^3$ echoes is compressed to $\bar{n} = 32$ elements.

in the optimisation problem to account for the variation in SNR associated with each element in **m**. Accordingly, Eq. (6) becomes

$$\mathbf{W}_0^{1/2}\mathbf{m} = \mathbf{W}_0^{1/2}\mathbf{K}_0\mathbf{f} + \mathbf{e}. \quad (7)$$

This means the calculated $\mathbf{K}_0$ will contain only $\sim 10^6$ elements.

We wish to determine a fitted solution vector $\hat{\mathbf{f}}$ that satisfies the non-negative least squares optimisation problem

$$\hat{\mathbf{f}} = \arg\min_{\mathbf{f} \geqslant 0} \left\| \mathbf{W}_0^{1/2}(\mathbf{m} - \mathbf{K}_0\mathbf{f}) \right\|^2, \quad (8)$$

where $\| \ldots \|$ is the ℓ_2 (Euclidean) norm of the vector. The matrix $\mathbf{K}_0$ is ill conditioned because there are more unknowns in the solution **f**

than there are knowns in the data **m**. This limitation is overcome by substituting the fitted solution vector $\hat{\mathbf{f}}$ with a vector of fitting parameters; in the maximum entropy method this vector is referred to as $\hat{\mathbf{a}}$ [18] and in Tikhonov regularisation this vector is referred to as $\hat{\mathbf{c}}$ [20]. Details of the mathematical methods for solving Eq. (8) can be found in the relevant literature [18–20,23] and are known to those familiar with this type of 2D relaxation and/or diffusion experiment. As such, we do not dwell on the specifics of the computation.

4. Experimental

The PFG-2SE experiments were conducted at a magnetic field strength of $B_0 = 0.042$ T corresponding to a resonant frequency of $\nu_0 = 1.93$ MHz for ^{1}H. Rf pulses of duration $t_{90} = 20$ μs and $t_{180} = 40$ μs were typical, corresponding to tip angles of 90° and 180° respectively. Sinusoidal gradient pulses were applied with a maximum gradient strength of $g_{\mathrm{PFG}} = 50$ G cm^{-1}, equivalent to a FFG of $g_{\mathrm{FFG}} = 31.8$ G cm^{-1}. For the validation of bulk water diffusivity, $g_{\mathrm{PFG}} = 30$ G cm^{-1}, equivalent to $g_{\mathrm{FFG}} = 19.1$ G cm^{-1}, was used to improve the sensitivity of the measurement to the high diffusion coefficient. The sample temperature was maintained at 25 °C at all times by the cooling water supply to the gradient coils. Eight dummy gradient pulses were applied prior to each scan to induce stable eddy currents in the magnet poles [24]. The gradient pulse durations were varied between $\delta_1 = 0.4$ ms and $\delta_{20} = 8$ ms. The required gradient stabilisation delay was 5 ms. Up to $n = 2 \times 10^4$ echoes were acquired with $t_{\mathrm{E}} = 600$ μs. In all cases, 11 complex data points were acquired with a dwell time of 1 μs from the top of each echo and averaged to improve the SNR.

The PFG-2SE pulse sequence is demonstrated on a selection of samples. The reference bulk liquids, doped water (0.1 mM Mn^{2+} solution) and synthetic oil S6 (viscosity standard manufactured by Cannon Instrument Company, USA), were placed between 2 mm diameter polytetrafluoroethylene (PTFE) spheres to reduce convection. Rock core-plugs of Bentheimer sandstone and Portland limestone were vacuum saturated with 2 wt.% KCl brine (used to prevent osmotic swelling of the clay content in the sandstone). The cylindrical core-plugs had dimensions of 60 mm × 38 mm (length × diameter). For these samples, 32 repeat scans were acquired for signal averaging and a SNR > 1000 was typical. The acquisition time for a complete 2D dataset ranged from 1 to 2 h depending on the recycle delay.

An example dataset acquired from the bulk water sample is shown in Fig. 5. The first row was obtained using the standard CPMG pulse sequence with $t_{\mathrm{E}} = 600$ μs (equivalent to $\delta_0 = 0$). The other rows of data were acquired using the PFG diffusion-editing pulse sequence. In Fig. 5, the first spin echo amplitudes are indicated by the × symbols. In logging tool diffusion-editing data, it is typical for the first echo intensity to be low compared to the second echo intensity as a consequence of applying rf pulses in the presence of a fixed field gradient [3]; this spin-dynamics phenomenon is not observed here. As the echo time increases, the temporal position of the spin echoes is seen to increase. This result highlights the irregular shape of the data when plotted against $t' = 2t_{\mathrm{SE},i} + nt_{\mathrm{E}}$. Only the second spin echo (2SE) and subsequent CPMG echoes are used in the numerical inversion.

In Section 2 we discussed the preferable use of the second spin echo (as opposed to the first) due to the inherent motion compensation. The quality of the diffusion decay can be assessed by plotting the normalised magnetisation (echo intensity) versus the b-factor. The diffusive decay of the first three echoes obtained from the bulk water sample is shown in Fig. 6. It is obvious that the second spin echo (∘) and subsequent CPMG echo (×) overlay well and exhibit an exponential decay, albeit a sum of the single component diffusion and relaxation exponents. The first spin echo (·), by contrast, does not overlay with the other echoes and exhibits a more complicated decay, possibly as a result of macroscopic sample motion (e.g. convection, mechanical vibration). However, as the attenuation per unit time is predominantly less for the first echoes than the second echoes, we note that this unintuitive result may suggest another explanation. We will consider the detailed spin dynamics of this experiment in future work. For now we conclude only that these results validate our decision to use the second spin echo for data processing.

In this work, we use Tikhonov regularisation with the optimum degree of smoothing estimated by the generalised cross validation (GCV) [25] method. Although in a comparison between well-logging data and a laboratory study it would be desirable to use the same inversion algorithm (e.g. the maximum entropy method), we found Tikhonov regularisation was more robust in the analysis of the PFG data presented here. Asymmetric eddy currents induced in the magnet poles following the gradient pulses resulted in slight systematic errors in the echo intensities; these eddy currents are a unique feature of the spectrometer system used and are not universal to all low-field benchtop magnets. The systematic errors in the data were sufficient to cause non-physical artifacts in the $D_{\mathrm{app}} - T_{2,\mathrm{eff}}$ correlations when fitted using the maximum entropy method. However, Tikhonov regularisation is less sensitive to these

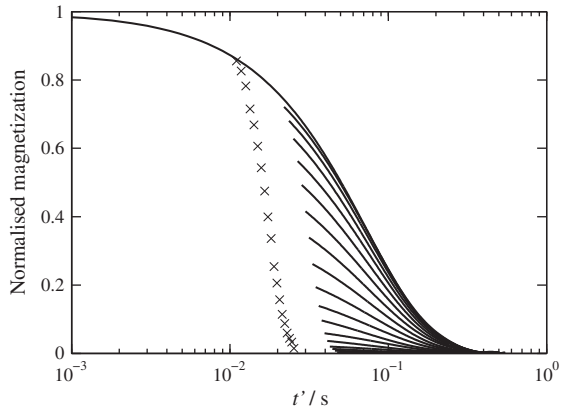

Fig. 5. Raw echo trains acquired using the PFG-2SE pulse sequence for doped water. The different decay curves (matrix rows) were acquired by varying the gradient pulse duration from $\delta_0 = 0$ to $\delta_{20} = 8$ ms (lines, top to bottom). The × symbols indicate the normalised magnetisation of the first spin echo.

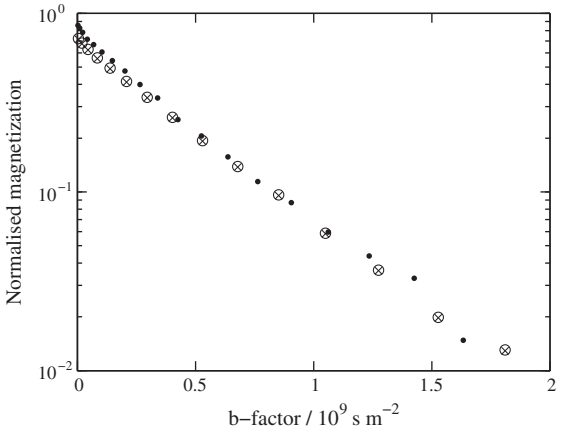

Fig. 6. Magnetisation of the first spin echo (·), the second spin echo (∘), and the first CPMG echo (×) acquired using the PFG-2SE pulse sequence with doped water. These echo intensities show an exponential dependence on b-factor as defined in Eq. (4).

errors; the degree of smoothing is increased by a small amount to account for the non-idealities in the data leading to a slight broadening of the 2D distribution, but artifacts are not present in the solution.

To demonstrate that the $D_{app} - T_{2,eff}$ correlations are quantitative, a model *in situ* oil recovery experiment was performed. Another Bentheimer sandstone core-plug (also of dimensions 60 mm × 38 mm) was saturated initially with dodecane. Doped brine (2 wt.% KCl and 0.1 mM Mn^{2+}) was used to displace the dodecane whilst the core-plug was mounted in a flow-through NMR compatible core-holder (ErgoTech, Conwy, UK). The manganese was chelated with ethylenediaminetetraacetic acid (EDTA) to prevent adsorption on clays. The brine was injected in 3 cm^3 increments, equivalent to 0.2 pore volumes (PV), where 1 PV = 15.3 cm^3. A $D_{app} - T_{2,eff}$ correlation was obtained between each brine injection, with only four repeat scans for signal averaging to provide a SNR < 100. Each 2D dataset was acquired in approximately 20 min; the factor of eight in reduction of experimental time was accompanied by a $\sqrt{8}$ reduction in SNR. The absolute SNR was reduced further by the presence of the electrically conductive brine in the flow channels of the NMR compatible core holder providing a path for rf interference that would be screened from the solenoid probe under normal operating conditions. The recovered effluent was analysed gravimetrically to determine the volumetric oil recovery for a comparison with the NMR results. To ensure the NMR results were quantitative in terms of liquid volume, calibration signal intensities were obtained from known volumes of brine and oil.

5. Results and discussion

Example $D_0 - T_2$ correlations for bulk liquids are shown in Fig. 7. The doped water, Fig. 7a, has a diffusivity of $D_0 = 2.26 \times 10^{-9}\ m^2\ s^{-1}$ as expected for water at ambient conditions. The T_2 is reduced from the usual relaxation time of $T_2 \approx 2$ s to $T_2 = 0.25$ s by the addition of the paramagnetic Mn^{2+} ions. Both the relaxation and diffusion distributions are single component so the $D_0 - T_2$ correlation exhibits a single narrow peak. By contrast, the $D_0 - T_2$ correlation of the S6 synthetic oil, Fig. 7b, provides a broader distribution of diffusion coefficients and relaxation times due to the variety of chemical components in this oil. The diffusion distribution spans the range $D_0 = 8 \times 10^{-11}$–$3 \times 10^{-10}\ m^2\ s^{-1}$. The distribution lies diagonally along the $D_0 - T_2$ correlation line predicted for bulk alkanes

$$D_0 \approx 5 \times 10^{-10} T_2, \tag{9}$$

as given in [2] where the empirical constant 5×10^{-10} has units $m^2 s^{-2}$. The log-mean diffusion coefficient of the S6 oil is $D_0 = 1.3 \times 10^{-10}\ m^2\ s^{-1}$ in agreement with previous diffusion studies of the same type of synthetic oil [2]; the log-mean $T_2 = 0.3$ s.

When confined in porous media, such as rock core-plugs, the diffusivity of water is reduced due to the restrictions imposed by the tortuous pore network. $D_{app} - T_{2,eff}$ correlations for brine in Portland limestone and Bentheimer sandstone are shown in Fig. 8a and b, respectively. The diffusion coefficient of the bulk brine is the same as that of bulk water. Both of these rocks are water-wet; thus the brine is expected to interact with the rock surface and move freely throughout the matrix. The brine in the Portland limestone, Fig. 8a, exhibits a bi-modal T_2 distribution corresponding to micropores and macropores for the short and long T_2 components, respectively. The diffusion coefficient of the brine in the macropores is $D_{app} = 2.15 \times 10^{-9}\ m^2\ s^{-1}$, whereas the diffusion coefficient of the brine confined in the micropores decreases as the $T_{2,eff}$ (and hence pore size) decreases. This result is consistent with the concept of restricted diffusion whereby the decreasing pore size limits the free diffusion path length of the water molecules, resulting in an apparent reduction in diffusion coefficient. The brine in the Bentheimer sandstone exhibits a single diffusion coefficient of $D_{app} = 2.23 \times 10^{-9}\ m^2\ s^{-1}$, Fig. 8b. This rock is known to have a mono-modal distribution of pore throat sizes ($R_{throat} \sim 10 - 100$ μm, determined by mercury intrusion porosimetry) and a predominantly mono-modal $T_{2,eff}$ distribution when measured at $\nu_0 = 2$ MHz [9]. The shorter relaxation time component observed at $T_{2,eff} \sim 0.1$ s could be evidence for regions of smaller porosity or water adsorbed on clays known to exist in small quantities in this sandstone. These clays give rise to susceptibility induced internal magnetic field gradients within the pores and evidence for these internal gradients, though weak, is visible in Fig. 8b in the form of signal artifacts at high diffusivity.

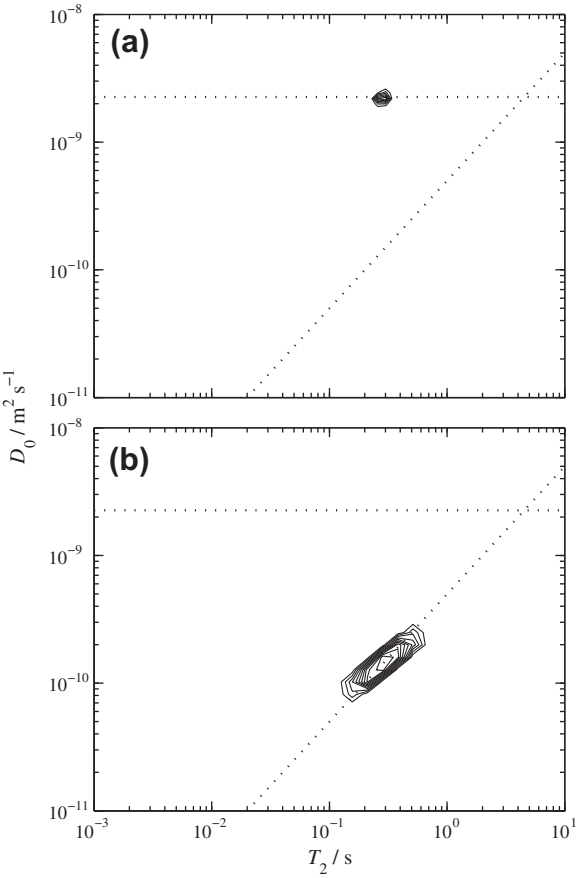

Fig. 7. $D_0 - T_2$ correlations for (a) doped water and (b) S6 oil acquired using the PFG-2SE sequence. In both plots, the horizontal dotted line indicates the diffusion coefficient of water at 25 °C and the diagonal dotted line indicates the $D_0 - T_2$ relationship for alkanes, Eq. (9).

When using laboratory $D_{app} - T_{2,eff}$ correlations to support well-logging data, it is imperative that a quantitative oil/brine saturation be obtained. To demonstrate the quantitative nature of the data, a model oil recovery experiment was conducted. An example $D_{app} - T_{2,eff}$ correlation measured during the brine flood of the Bentheimer sandstone core-plug saturated initially with dodecane is shown in Fig. 9a. This dataset was obtained after 15 $cm^3 \equiv 1$ PV brine had been injected. The injection rate was high, so the brine fingered through the dodecane, leaving a significant volume of oil remaining despite the rock surface being nominally water-wet. As discussed in Section 4, the SNR was reduced in this study compared to the results shown in Figs. 7 and 8. Hence the peaks in the 2D distribution in Fig. 9a are broadened significantly and do not exhibit any fine detail pertaining to the pore matrix. However, because the brine relaxation is controlled by the chelated dopant

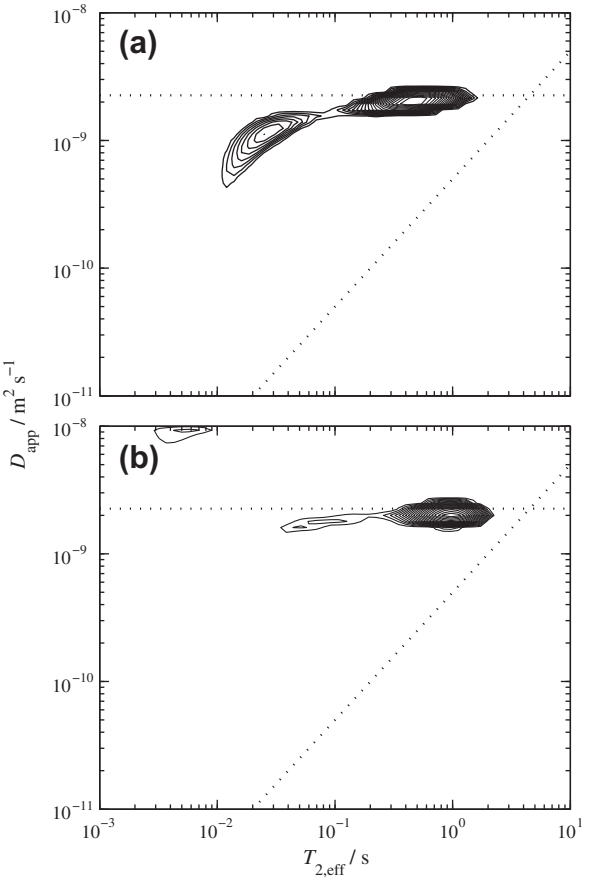

Fig. 8. $D_{app} - T_{2,eff}$ correlations for (a) Portland limestone and (b) Bentheimer sandstone saturated with 2 wt.% KCl brine. In (b) a signal artifact is observed at high diffusivities due to internal gradients in the sandstone. In both plots, the horizontal dotted line indicates the diffusion coefficient of water at 25 °C and the diagonal dotted line indicates the $D_0 - T_2$ relationship for alkanes, Eq. (9).

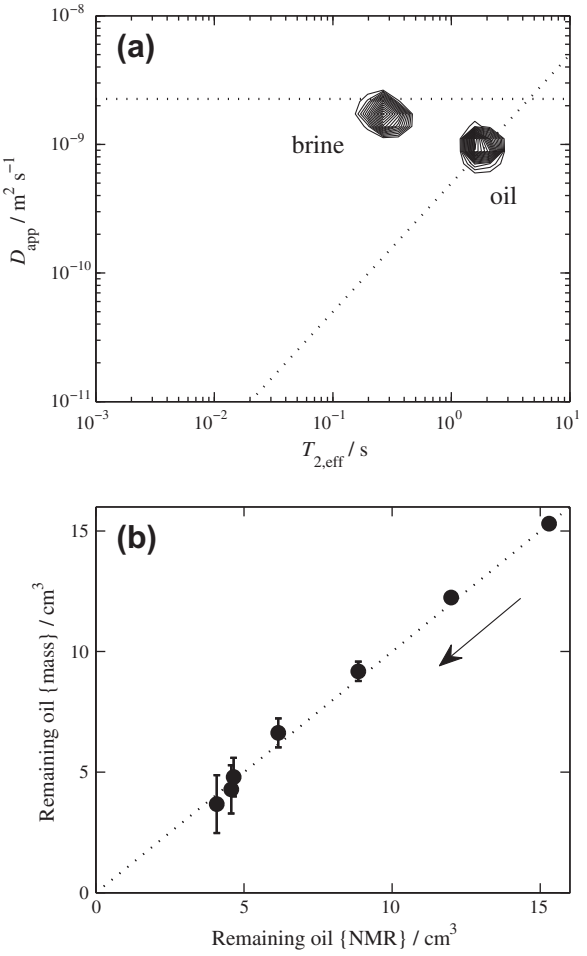

Fig. 9. Demonstration of quantitative oil recovery monitoring. (a) $D_{app} - T_{2,eff}$ correlation for the Bentheimer sandstone core-plug, saturated initially with dodecane (oil), following the injection of 15 cm^3 doped brine. (b) A comparison of dodecane remaining in the core-plug as determined gravimetrically and by NMR. Error bars are explained in the text. The arrow indicates the order in which the data were acquired as the brine injection progressed. The diagonal dotted line indicates volumetric equality.

and the oil has a very weak interaction with the water-wet surface, it is not unreasonable to expect an insensitivity to local geometry in the T_2 distribution. The apparent diffusion coefficient of the brine is still reduced when compared to the bulk diffusion coefficient of water. The dodecane peak remains on the alkane line because the bulk diffusion coefficient of the oil is sufficiently low as to be insensitive to the confinement in the large pores of this sandstone. Despite the broadening of the peaks, the oil and brine signals are well separated allowing an independent determination of the oil and brine volumes. The peak areas were integrated and scaled using the calibration hydrogen-indices to determine the remaining oil and brine in the core-plug at each stage of the flood.

The NMR results are compared to the gravimetric estimates of remaining oil in Fig. 9b where excellent agreement between the two sets of data is observed. The errors on the NMR determination of oil volume are considered to be small (within the bounds of the markers). The errors on the gravimetric estimate are also small, but cumulative as the effluent is assessed after each brine injection. The remaining oil saturation achieved at the end of this flood was S_{ro} = 25%. The inclusion of the zeroth column in the PFG-2SE sequence ensures the total signal intensity in the $D_{app} - T_{2,eff}$ correlation retains the same level of accuracy as a 1D $T_{2,eff}$ distribution. These additional data mean the volumes extracted from this diffusion editing sequence are more quantitative than from, say, a stimulated echo PFG experiment where an unknown degree of T_1 relaxation will have occurred prior to the acquisition of the first echo even when the pulse gradient amplitude is set to zero. The PFG-2SE measurement therefore has a distinct advantage over other PFG techniques, especially when examining short T_2 and T_1 materials, such as heavy oils.

The simultaneous determination of the oil and brine volumes present in the core-plug provides the NMR method with an advantage over traditional gravimetric oil recovery monitoring techniques where the remaining oil saturation is estimated based on the oil recovered. Furthermore, the brine saturation can be determined gravimetrically only by assuming the core-plug remains fully saturated with liquid. The NMR measurements, being independent and quantitative assessments of the absolute liquid volume in the core-plug, will be able to detect a reduction in total liquid volume due to gas trapped in the pores.

6. Conclusions

In this paper we have described the implementation of a PFG pulse sequence that emulates the FFG sequence used on unilateral NMR devices, such as oil well-logging tools. Therefore, the PFG sequence allows a direct comparison of $D_{app} - T_{2,eff}$ correlations obtained in the laboratory with those obtained in a well-logging study. Example datasets have been presented, including bulk water and oil samples, as well as brine saturated sandstone and limestone core-plugs. The quantitative nature of the $D_{app} - T_{2,eff}$ correlations was demonstrated by monitoring a model oil recovery

experiment, where excellent agreement was observed between the NMR and gravimetric estimates of remaining oil. The NMR data also provide a quantitative assessment of the brine content of the core-plug that cannot be obtained readily using traditional gravimetric effluent analysis.

Diffusion-editing data requires a little more care at the numerical inversion stage than most 2D relaxation or diffusion correlations due to the shared time variable in the two dimensions of the experiment. Notwithstanding, this $D - T_2$ correlation provides quantitative data with less signal loss due to relaxation weighting than in more conventional stimulated echo PFG pulse sequences. The PFG-2SE sequence described here is suitable for laboratory-scale studies of porous materials and short T_2 samples in general.

Acknowledgements

The authors thank Mr. John Staniland and Mr. Alex Wilson for assistance with the sample preparation, and Mr. Thusara Chandrasekera for assistance with the numerical inversion algorithms. For financial support the authors thank Schlumberger Cambridge Research.

References

[1] R.L. Kleinberg, Data interpretation and reservoir analysis, Concept. Magn. Reson. 13A (2001) 404–406.
[2] M.D. Hürlimann, L. Venkataramanan, C. Flaum, The diffusion-spin relaxation time distribution function as an experimental probe to characterize fluid mixtures in porous media, J. Chem. Phys. 117 (2002) 10223–10232.
[3] M.D. Hürlimann, L. Venkataramanan, Quantitative measurement of two-dimensional distribution functions of diffusion and relaxation in grossly inhomogeneous fields, J. Magn. Reson. 157 (2002) 31–42.
[4] S. Arora, D. Horstmann, P. Cherukupalli, J. Edwards, R. Ramamoorthy, T. McDonald, D. Bradley, C. Ayan, J. Zaggas, K. Cig, Single-well in-situ measurement of residual oil saturation after an EOR chemical flood, SPE 129069.
[5] P.J. McDonald, Stray field magnetic resonance imaging, Prog. Nucl. Magn. Reson. Spectrosc. 30 (1997) 69–99.
[6] J. Mitchell, P. Blümler, P.J. McDonald, Spatially resolved nuclear magnetic resonance studies of planar samples, Prog. Nucl. Magn. Reson. Spectrosc. 48 (2006) 161–181.
[7] J. Mitchell, E.J. Fordham, A system and method for emulating nuclear magnetic resonance well-logging tool diffusion editing measurements on a bench-top nuclear magnetic resonance spectrometer for laboratory-scale rock core analysis, US patent application 12/731,005; Publication pending September 2011, 2010.
[8] G. Leu, E.J. Fordham, M.D. Hürlimann, P. Frulla, Fixed and pulsed gradient diffusion methods in low-field core analysis, Magn. Reson. Imaging 23 (2005) 305–309.
[9] J. Mitchell, T.C. Chandrasekera, M.L. Johns, L.F. Gladden, E.J. Fordham, Nuclear magnetic resonance relaxation and diffusion in the presence of internal gradients: the effect of magnetic field strength, Phys. Rev. E 81 (2010) 026101.
[10] W.S. Price, Pulsed-field gradient nuclear magnetic resonance as a tool for studying translational diffusion: part I. Basic theory, Concept. Magn. Reson. 9A (1997) 299–336.
[11] W.S. Price, Pulsed-field gradient nuclear magnetic resonance as a tool for studying translational diffusion: part II. Experimental aspects, Concept. Magn. Reson. 10A (1998) 197–237.
[12] R.M. Cotts, M.J.R. Hoch, T. Sun, J.T. Marker, Pulsed field gradient stimulated echo methods for improved NMR diffusion measurements in heterogeneous systems, J. Magn. Reson. 83 (1989) 252–266.
[13] J.E. Tanner, Use of stimulated echo in NMR-diffusion studies, J. Chem. Phys. 52 (1970) 2523–2526.
[14] E.D. Stejskal, J.E. Tanner, Spin diffusion measurements: spin echoes in the presence of a time-dependent field gradient, J. Chem. Phys. 42 (1965) 288–292.
[15] H. Carr, E. Purcell, Effects of diffusion on free precession in NMR experiments, Phys. Rev. 94 (1954) 630–638.
[16] S. Meiboom, D. Gill, Modified spin-echo method for measuring nuclear relaxation times, Rev. Sci. Instrum. 29 (1958) 668–691.
[17] M.D. Hürlimann, Optimization of timing in the Carr–Purcell–Meiboom–Gill sequence, Magn. Reson. Imaging 19 (2001) 375–378.
[18] N.J. Heaton, Multi-measurement NMR analysis based on maximum entropy, US patent 6,960,913 B2, 2005.
[19] J.P. Butler, J.A. Reeds, S.V. Dawson, Estimating solutions of 1st kind integral-equations with nonnegative constraints and optimal smoothing, SIAM J. Numer. Anal. 18 (3) (1981) 381–397.
[20] L. Venkataramanan, Y.Q. Song, M.D. Hürlimann, Solving Fredholm integrals of the first kind with tensor product structure in 2 and 2.5 dimensions, IEEE Trans. Sig. Process. 50 (2002) 1017–1026.
[21] M. Flaum, Fluid and rock characterization using new NMR diffusion-editing pulse sequences and two dimensional diffusivity-T_2 maps, Ph.D. thesis, Rice University, 2006.
[22] B. Sun, K.J. Dunn, Method for obtaining multi-dimensional proton density distributions from a system of nuclear spins, US patent 6,937,014 B2, 2005.
[23] J. Mitchell, T.C. Chandrasekera, L.F. Gladden, Obtaining true transverse relaxation time distributions in high-field NMR measurements of saturated porous media: removing the influence of internal gradients, J. Chem. Phys. 132 (2010) 244705.
[24] S.J. Gibbs, C.S. Johnson, A PFG NMR experiment for accurate diffusion and flow studies in the presence of eddy currents, J. Magn. Reson. 93 (1991) 395–402.
[25] G. Wahba, Practical approximate solutions to linear operator equations when data are noisy, SIAM J. Numer. Anal. 14 (1977) 651–667.